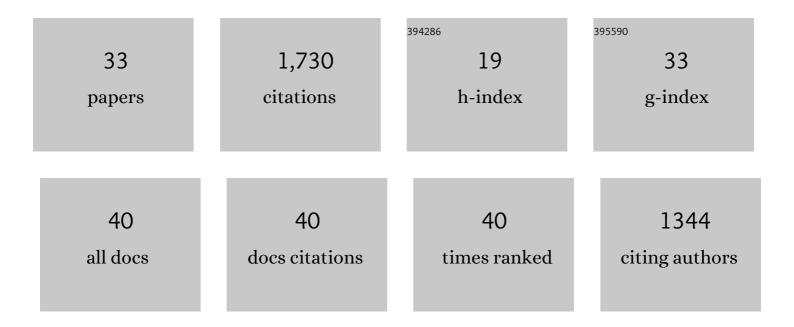
Laurentiusâ€[−] Huber

List of Publications by Year in descending order

Source: https://exaly.com/author-pdf/3971479/publications.pdf Version: 2024-02-01



#	Article	IF	CITATIONS
1	High-Resolution CBV-fMRI Allows Mapping of Laminar Activity and Connectivity of Cortical Input and Output in Human M1. Neuron, 2017, 96, 1253-1263.e7.	3.8	255
2	Cortical lamina-dependent blood volume changes in human brain at 7 T. NeuroImage, 2015, 107, 23-33.	2.1	152
3	Layer-dependent activity in human prefrontal cortex during working memory. Nature Neuroscience, 2019, 22, 1687-1695.	7.1	130
4	Slab-selective, BOLD-corrected VASO at 7 Tesla provides measures of cerebral blood volume reactivity with high signal-to-noise ratio. Magnetic Resonance in Medicine, 2014, 72, 137-148.	1.9	107
5	Investigation of the neurovascular coupling in positive and negative BOLD responses in human brain at 7T. NeuroImage, 2014, 97, 349-362.	2.1	101
6	Techniques for blood volume fMRI with VASO: From low-resolution mapping towards sub-millimeter layer-dependent applications. NeuroImage, 2018, 164, 131-143.	2.1	101
7	Non-BOLD contrast for laminar fMRI in humans: CBF, CBV, and CMRO2. NeuroImage, 2019, 197, 742-760.	2.1	96
8	Sub-millimeter fMRI reveals multiple topographical digit representations that form action maps in human motor cortex. NeuroImage, 2020, 208, 116463.	2.1	88
9	Layer-dependent functional connectivity methods. Progress in Neurobiology, 2021, 207, 101835.	2.8	67
10	Lamina-dependent calibrated BOLD response in human primary motor cortex. NeuroImage, 2016, 141, 250-261.	2.1	66
11	LayNii: A software suite for layer-fMRI. NeuroImage, 2021, 237, 118091.	2.1	64
12	Layer-specific activation of sensory input and predictive feedback in the human primary somatosensory cortex. Science Advances, 2019, 5, eaav9053.	4.7	62
13	Ultra-high resolution blood volume fMRI and BOLD fMRI in humans at 9.4†T: Capabilities and challenges. NeuroImage, 2018, 178, 769-779.	2.1	44
14	Baseline oxygenation in the brain: Correlation between respiratory-calibration and susceptibility methods. NeuroImage, 2016, 125, 920-931.	2.1	35
15	Layer-Specific Contributions to Imagined and Executed Hand Movements in Human Primary Motor Cortex. Current Biology, 2020, 30, 1721-1725.e3.	1.8	35
16	Vascular autorescaling of fMRI (VasA fMRI) improves sensitivity of population studies: A pilot study. NeuroImage, 2016, 124, 794-805.	2.1	33
17	Comparison of BOLD and CBV using 3D EPI and 3D GRASE for cortical layer functional MRI at 7 T. Magnetic Resonance in Medicine, 2020, 84, 3128-3145.	1.9	33
18	Sub-millimetre resolution laminar fMRI using Arterial Spin Labelling in humans at 7 T. PLoS ONE, 2021, 16, e0250504.	1.1	27

Laurentiusâ€[−] Huber

#	Article	IF	CITATIONS
19	Cortical laminar restingâ€state signal fluctuations scale with the hypercapnic blood oxygenation levelâ€dependent response. Human Brain Mapping, 2020, 41, 2014-2027.	1.9	25
20	Optimization of simultaneous multislice EPI for concurrent functional perfusion and BOLD signal measurements at 7T. Magnetic Resonance in Medicine, 2017, 78, 121-129.	1.9	24
21	Functional cerebral blood volume mapping with simultaneous multi-slice acquisition. NeuroImage, 2016, 125, 1159-1168.	2.1	22
22	Higher and deeper: Bringing layer fMRI to association cortex. Progress in Neurobiology, 2021, 207, 101930.	2.8	21
23	Regional reproducibility of calibrated BOLD functional MRI: Implications for the study of cognition and plasticity. NeuroImage, 2014, 101, 8-20.	2.1	18
24	Linking cortical circuit models to human cognition with laminar fMRI. Neuroscience and Biobehavioral Reviews, 2021, 128, 467-478.	2.9	17
25	Challenges and opportunities of mesoscopic brain mapping with fMRI. Current Opinion in Behavioral Sciences, 2021, 40, 189-200.	2.0	15
26	Anatomical brain imaging at 7T using twoâ€dimensional GRASE. Magnetic Resonance in Medicine, 2014, 72, 1291-1301.	1.9	12
27	Fast accurate MR thermometry using phase referenced asymmetric spinâ€echo EPI at high field. Magnetic Resonance in Medicine, 2014, 71, 524-533.	1.9	12
28	Layer-specific activation in human primary somatosensory cortex during tactile temporal prediction error processing. Neurolmage, 2022, 248, 118867.	2.1	11
29	Using carbogen for calibrated fMRI at 7Tesla: Comparison of direct and modelled estimation of the M parameter. NeuroImage, 2014, 84, 605-614.	2.1	9
30	Simultaneous acquisition of cerebral blood volumeâ€, blood flowâ€, and blood oxygenationâ€weighted <scp>MRI</scp> signals at ultraâ€high magnetic field. Magnetic Resonance in Medicine, 2015, 74, 513-517.	1.9	9
31	Physiological basis of vascular autocalibration (Vas <scp>A</scp>): Comparison to hypercapnia calibration methods. Magnetic Resonance in Medicine, 2017, 78, 1168-1173.	1.9	7
32	Concurrent CBF and BOLD fMRI with dual-echo spiral simultaneous multi-slice acquisitions at 7T. NeuroImage, 2022, 247, 118820.	2.1	5
33	Magnetization transfer weighted EPI facilitates cortical depth determination in native fMRI space. NeuroImage, 2021, 242, 118455.	2.1	4